

# Trajectory Specification for Accurate Tracking Control of a Differential Drive WMR

J Garbutt

*School of Aerospace, Mechanical  
& Manufacturing Engineering,  
RMIT University, PO Box 71,  
Bundoora, Australia 3083.  
jlgarbutt@hotmail.com*

S John

*School of Aerospace, Mechanical  
& Manufacturing Engineering,  
RMIT University, PO Box 71,  
Bundoora, Australia 3083.  
sabu.john@rmit.edu.au*

T Vinay

*School of Electrical and  
Computer Systems Engineering,  
RMIT University GPO Box  
2476V, Melbourne, Australia,  
3001.  
thurai@rmit.edu.au*

## Abstract

*As the speed and payload of Wheeled Mobile Robots (WMRs) increases and the clearances between obstacles and docking error tolerances decreases, methods for reducing tracking errors become increasingly important for a successful application. In this paper techniques and results are presented for improved tracking control of a WMR through the generation and dynamic simulation of paths with and without curvature discontinuities.*

**Keywords:** Wheeled mobile robot, simulation, control, trajectory, dynamic, wheel slip.

## 1. Introduction

Wheeled Mobile Robots (WMRs), also known as automated guided vehicles (AGVs) have a long history, and with the substantial growth of automation in manufacturing and assembly they are becoming an increasingly important element in integrated systems. WMR technology began with a generation of fixed path systems, which still constitute the majority of WMR systems in operation today, employing optical, capacitive, inductive or other sensors. The trajectories to be followed commonly take the form of a white line, a metallic strip or a chemical trail on the floor, or a current-carrying wire embedded in the floor. Thus, as long as routes are well established and do not need to change frequently, the aforementioned path following systems offer accurate and reliable material transportation at relatively low cost. Such systems however are not considered to be truly "autonomous".

With advances in technology, the present generation of WMRs is based on open path methods and is able to navigate freely on any part of the factory floor cognizant of the physical environment and the motion requirements. Replacing the physical guide paths of fixed path systems with software

control has given WMRs more flexibility and capability.

Many software based hierarchical control systems have been proposed and implemented for experimental WMRs. At the highest level, the path planner utilizes the most recent map of the environment to plan a collision free path for the WMR. The planned path can be constrained by the kinematic characteristics of the WMR. The trajectory planner then associates with the path, a schedule according to WMR dynamic characteristics. This association is named trajectory. A velocity profile is then assigned to the path, giving the desired trajectory in the world coordinates. The trajectory is passed to the lower level control system, which continuously monitors the state of the WMR and evaluates and issues appropriate control signals to the robots motion actuators.

In this paper we are concerned with the problem of specifying and generating practicable path and trajectory data for the accurate tracking control of differentially steered WMRs. In the literature, there have been a number of theories for planning paths for WMR navigation [1, 2, 3]. In general, we can consider two methods of path description for WMRs [3]: i) A path may be implicitly specified by giving a sequence of postures  $(x, y, \theta)$  and a local path-solver used to find a path segment joining two adjacent postures; or ii) A path may be specified as a sequence of explicitly defined path segments where both end points  $(x, y, \theta)$ , and other parameters, including the radius of a circle, or the focus of a parabola, and others, are needed to define each path segment.

For the aforementioned theories a typical class of planned paths comprises a list of path segments of two basic types: straight-line segments and arcs, which are connected so that the resultant path has tangent direction continuity. The primary reason for the pervasive use of this class of path is that it has been shown that the shortest path for a car-like robot between two configurations is such a path [4]. The secondary reason is that these paths are easy to deal with from a computational point of view [5]. Paths

having tangent direction continuity are referred to in [3] as class 2 type paths.

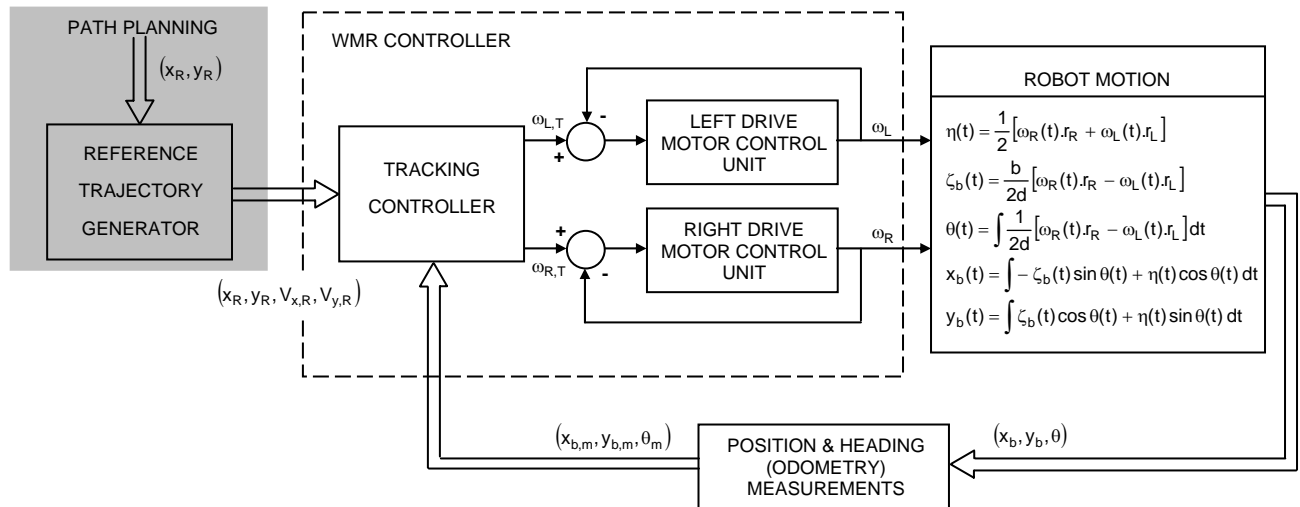


Figure 1. Block diagram of basic WMR tracking control architecture with path planner

However, it is well known by researchers that the curvature of class 2 paths is discontinuous; the discontinuities occurring at the transitions between straight-line and arc segments. It has also been shown that the rotational velocity of each drive wheel of a differentially steered WMR is a linear function of the path curvature and as a consequence these discontinuities may invoke the robot dynamics resulting in wheel slip and tracking errors. While it is possible to make these tracking errors transient in nature through proper error sensing and feedback control, as the speed and payload of WMRs increases and the clearances between obstacles and docking error tolerances decrease, methods for reducing these errors through the elimination of path curvature discontinuities become increasingly important.

Class 3 paths are the smoothest and most suitable for WMR path planning having tangent direction and curvature continuity. In a survey of the available literature, class 3 paths have been studied by several authors and include quintic polynomial curves [5], cubic spirals [6], and clothoids curves [7, 8]. Many previous papers on class 3 paths have concentrated on path planning and generation but have stopped short of trajectory planning using velocity profiles. In [7] Konishi reports on the path generation and velocity control of an autonomous steered wheel vehicle in which the path is implicitly specified by giving a sequence of postures and a local path-solver is used to interpolate between two adjacent postures using clothoid curves and straight line segments.

In this paper a local trajectory-planning algorithm for a differentially steered WMR is presented in which the path is specified as a sequence of explicitly defined segments using circular arcs, clothoid curves and straight-lines. Trapezoidal velocity profiles are then assigned to the segments taking into account the inherent kinematic and dynamic constraints of the WMR.

## 2. Preliminaries

Whilst the work presented in this paper may be applied to WMRs assuming a number of different mechanical drive configurations, in light of the current research effort, we formulate the problem in terms of the key position and orientation variables of a differentially steered WMR restricted to planar motion. A block diagram of typical WMR tracking control architecture is presented in Figure 1. The interested reader may also refer to [9] for details of kinematic and dynamic model formulation for simulation results presented herein. WMR parameters are as per [9].

### 2.3. Problem Formulation

The impetus behind the work presented in this paper is concerned with the development of control algorithms for the accurate tracking control of differentially steered WMRs. In the tracking control problem, an essential component involves the specification and generation of practicable path and trajectory data, which takes into consideration the kinematic and dynamic constraints of the vehicle. In the following sections we will provide details of software algorithms developed for class 2 and 3 type paths in Simulink® for the accurate path planning and trajectory planning of a differential drive WMR. Finally, simulation results for each class are presented and compared and recommendations made.

Our approach to path planning is to generate a 2D class 2 or 3 type path in an inertial Cartesian coordinate frame that is fixed to the WMR at the midpoint of the baseline. Granted that the path is of type 2 or 3 the nonholonomic path constraints, which arise from the mechanical configuration of the

WMR, will be inherently satisfied. If the path constraints are violated, the path cannot be followed at higher speeds and in many cases will require that the robot stop at successive path segments to change its orientation. It is important to note that an implicit assumption in WMR planning is that no slippage occurs at the wheel contact point [2]. Given a feasible path, a trajectory for the midpoint of the WMR's baseline is generated by assigning a desired velocity profile. The trajectory is evaluated against the relevant kinematic variables (velocities and accelerations) and operational limits to generate a velocity profile, which satisfies kinematic constraints. The required control inputs and frictional forces are simulated and compared to dynamic constraints. When the kinematic and dynamic constraints are satisfied, the trajectory can be successfully executed by the WMR.

### 3. Path Specification & Planning Requirements

In the approach that follows, the path is specified as a sequence of explicitly defined path segments where the initial configuration  $(x_b, y_b, \theta)$ , and other parameters, including the radius of a circle, the distance to be traveled, and others are needed to define each path segment. For simplicity, it is commonly assumed that the tracking point is located on the baseline ( $P_b = 0$ ) of the WMR for path planning purposes. This assumption is applied in the following analysis.

Also the type of robot being implemented places particular (nonholonomic) constraints on its feasible motion. These must be accounted for when planning techniques are developed to ensure that accurate and close path tracking is possible.

#### 3.1. Straight-line Path Segments

In defining path segments comprising of straight-line motions it is necessary to explicitly define the initial posture  $(x_{b,i}, y_{b,i}, \theta_i)$  and the distance to be travelled  $s$ .

#### 3.2 Circular Arc Path Segments

In defining a circular arc path segment, in which  $|\Delta\theta|$  is restricted to  $\leq 180$  per segment, it is necessary to explicitly specify the radius of curvature  $\rho$ , initial posture  $(x_{b,i}, y_{b,i}, \theta_i)$ , final orientation  $\theta_f$  and the direction of rotation  $\delta$ .

For user inputs and calculations involving angles and their addition and subtraction a 180 to -180 degrees 'wraparound check' is carried out to ensure the angles remain in the bounds defined above. The 'wraparound check' performed for user inputs  $\theta_{i,p}$  and  $\theta_{f,p}$ , the subscript lowercase p denotes pre-checked inputs,

For  $\theta_{j,p} > 180$ ,  $\theta_j = \theta_{j,p} - 360$  where  $(j = i, f)$

For  $\theta_{j,p} < -180$ ,  $\theta_j = \theta_{j,p} + 360$

(1)

For  $-180 \leq \theta_{j,p} \leq 180$ ,  $\theta_j = \theta_{j,p}$

The total path segment distance to be travelled  $s$  is simply calculated by  $s = 2\pi\rho(\theta_{f,p} - \theta_{i,p})/360$

The orientation of the WMR at any distance along the circular arc segment for clockwise rotation ( $\delta = -1$ ) and anti-clockwise rotation ( $\delta = 1$ ) is calculated as,  $\theta(s) = \theta_{i,p} - \delta s/\rho$ .

The total change in orientation of the WMR is calculated as  $\Delta\theta_p = \theta_{f,p} - \theta_{i,p}$ . Applying the 'wraparound check' the change in orientation  $\Delta\theta$  is,

For  $\Delta\theta_p > 180$ ,  $\Delta\theta = \Delta\theta_p - 360$

For  $\Delta\theta_p < -180$ ,  $\Delta\theta = \Delta\theta_p + 360$

(2)

For  $-180 \leq \Delta\theta_p \leq 180$ ,  $\Delta\theta = \Delta\theta_p$

The angles,  $\phi_i$  and  $\phi_f$ , which are required to establish the change in position of the robot along the arc are,

For  $|\Delta\theta_p| = 180$ ,  $\phi_i = \theta_{i,p} - 90\delta$ ,  $\phi_f = \theta_{f,p} - 90\delta$

For  $|\Delta\theta_p| \neq 180$ ,

(3)

$\phi_i = \theta_{i,p} - 90 \text{sgn}(\Delta\theta_p)$ ,  $\phi_f = \theta_{f,p} - 90 \text{sgn}(\Delta\theta_p)$

The change in position of the robot in x and y coordinates is defined in (4) and the position of the robot along the circular arc in (5),

$$\Delta x_b = \rho(\cos \phi_f - \cos \phi_i), \Delta y_b = \rho(\sin \phi_f - \sin \phi_i) \quad (4)$$

$$x_b = \Delta x_b + x_{b,i},$$

$$y_b = \Delta y_b + y_{b,i}$$

(5)

### 4. Trajectory Planning with a Velocity Profile

In industrial and manufacturing applications, time and speed are very important parameters when calculating the productivity and efficiency of a process. Hence, in the trajectory tracking control problem it is a requirement that the WMR be able to track a time-indexed trajectory. In such cases motion control is commonly achieved with a velocity profile. The trapezoidal profile considered to be the most practical of the velocity profiles. Consisting of the three time can be set in any number of ways, the profile is typically

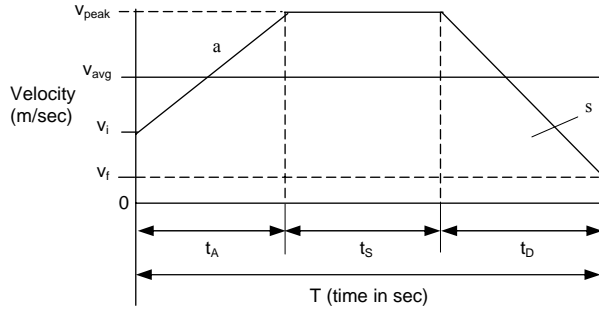


**Figure 2. Trapezoidal Velocity Profile**

intervals of acceleration, slew and deceleration, which defined by the three time intervals being equal to one-third of the motion time.

Whilst setting  $t_A = t_s = t_D$  greatly simplifies the analysis for longer distances of travel this profile may not always be the most appropriate. Hence a general form of the above equations is derived as shown in Figure 2.

The trapezoidal velocity profile embodies important information for path planning. The distance travelled ( $s$ ) is equal to the integral of the velocity profile written as,

$$s = \frac{1}{2} [v_{\text{peak}} \cdot (t_A + 2t_s + t_D) + v_i \cdot t_A + v_f \cdot t_D] \quad (6)$$

The peak velocity ( $v_{\text{peak}}$ ) is equal to the highest or lowest point over the entire curve and is calculated as,

$$v_{\text{peak}} = (2s - v_i \cdot t_A - v_f \cdot t_D) / (t_A + 2t_s + t_D) \quad (7)$$

For the acceleration period  $0 \leq t \leq t_A$  and deceleration period  $(T - t_D) \leq t \leq T$  respectively, we calculate the accelerations as,

$$a(t) = \frac{v_{\text{peak}} - v_i}{t_A} = \frac{2s - v_i \cdot t_A - v_f \cdot t_D}{t_A(t_A + 2t_s + t_D)} - \frac{v_i}{t_A} \quad (8)$$

$$a(t) = \frac{v_{\text{peak}} - v_f}{t_D} = \frac{2s - v_i \cdot t_A - v_f \cdot t_D}{t_D(t_A + 2t_s + t_D)} - \frac{v_f}{t_D} \quad (9)$$

To alleviate some of the computations required in the path planning process, specifying an acceleration rate or maximum acceleration of the robot makes possible the automatic generation of the time periods in terms of the velocity parameters. From equations (6)–(9) we can express the motion time as,

$$T = \frac{2v_{\text{peak}}(v_{\text{peak}} - v_f - v_i) + 2sa_{\text{max}} + v_i^2 + v_f^2}{2v_{\text{peak}}a_{\text{max}}} \quad (10)$$

By specifying the acceleration rate and initial and final velocities, there exists a finite range  $T_{\text{min}} \leq T < T_{\text{max}}$  for which the motion time ( $T$ ) yields a valid profile. The minimum motion time ( $T$ ) occurs when we accelerate from  $v_i$  to  $v_{\text{max}}$  and decelerate from  $v_{\text{max}}$  to  $v_f$  at maximum acceleration. / deceleration Substituting  $v_{\text{max}}$  into equation (10) we get (11),

$$T_{\text{min}} = \frac{2v_{\text{max}}(v_{\text{max}} - v_f - v_i) + 2sa_{\text{max}} + v_i^2 + v_f^2}{2v_{\text{max}}a_{\text{max}}}$$

The maximum travel time ( $T$ ) occurs when the peak velocity is equal to the greater of  $v_i$  or  $v_f$ . Substituting  $v_i$  and  $v_f$  into equation (10) respectively we get (12),

$$T_{\text{max}} = \min \left( \frac{2sa_{\text{max}} + (v_i - v_f)^2}{2v_i a_{\text{max}}}, \frac{2sa_{\text{max}} + (v_i - v_f)^2}{2v_f a_{\text{max}}} \right)$$

The time periods  $t_A$  and  $t_D$  are calculated from (8) and (9) and  $t_s$  from,  $t_s = T - (2v_{\text{peak}} + v_i + v_f) / a_{\text{max}}$ . From equations (7), (8) and (9), the peak velocity is

$$v_{\text{peak}} = \frac{1}{2} \left[ \frac{(Ta_{\text{max}} + v_f + v_i)}{\sqrt{(-Ta_{\text{max}} - v_f - v_i)^2 - (4sa_{\text{max}} - 2v_i^2 - 2v_f^2)}} \right] \quad (13)$$

## 4.2 Planning with Sections of the Profile

Path planning with selected sections of the trapezoidal profile is considered where one or two of  $t_A$ ,  $t_s$  and  $t_D = 0$ . Such profiles are useful in executing speed constrained manoeuvres such as cornering and work station docking.

### 4.2.1 Constant Velocity Profile

Referring to figure 2 for motions requiring constant velocity,  $t_s = T$  and  $v_{\text{peak}} = v_i = v_f$ . Constant velocity profiles are often associated with planning cornering speeds and curvilinear motions where  $T = s/v_i = t_s$ .

### 4.2.2 Acceleration / Slew Profile

For path planning tasks requiring acceleration from an initial velocity to a constant velocity (final velocity) a profile is defined where  $t_s + t_A = T$  and  $v_{\text{peak}} = v_f$ . This profile is also often associated with

planning curvilinear motions and the commencement of a profile. The profile is valid for  $T_{\min} \leq T < T_{\max}$ ,

$$\frac{2a_{\max}s + (v_f - v_i)^2}{2a_{\max}v_f} \leq T < \frac{2s}{(v_f + v_i)} \quad (14)$$

where  $T_{\min}$  occurs for maximum acceleration from  $v_i$  to  $v_f$  and  $T_{\max}$  for  $t_A = T$ . The time periods are defined using (6) with  $t_D = 0$  as follows,

$$t_S = T - [2(s - v_f T)] / (v_i - v_f) \quad (15)$$

#### 4.2.3 Slew / Deceleration Profile

For path planning requiring constant velocity at an initial velocity and deceleration to a final velocity, a profile is defined where  $t_S + t_D = T$  and  $v_{\text{peak}} = v_i$ . This profile is often associated with planning curvilinear motions and for closing a profile. The profile is valid for  $T_{\min} \leq T < T_{\max}$ ,

$$\frac{2a_{\max}s + (v_f - v_i)^2}{2a_{\max}v_i} \leq T < \frac{2s}{(v_f + v_i)} \quad (16)$$

where the minimum travel time  $T_{\min}$  occurs for maximum deceleration from  $v_i$  to  $v_f$  and  $T_{\max} t_D = T$ . The time periods are defined using (6) with  $t_A = 0$  as,

$$t_S = T - [2(s - v_i T)] / (v_f - v_i) \quad (17)$$

### 4.3 Velocity and Acceleration Limits

The time periods of the profile are generated from  $a_{\max}$ . The maximum acceleration specified by the path planner can take on the value of actuator limitations or limits imposed by other considerations such as payload or operating conditions. Limitations on the maximum velocity of the robot are applied whereby the peak value of the profile is limited to  $v_{\text{peak}} \leq v_{\max}$ .

### 4.4 Generating the Trajectory Parameters

From the velocity profile function the path planning data is generated based on  $\theta(t)$  for the specified path type. For straight line path  $\theta(t) = \theta_{i,p}$  and for circular arc path we utilise the distance function to calculate  $\theta(t) = \theta_{i,p} + \delta s(t) / \rho$ . The path data is,

$$v_{x\text{Ref}}(t) = v(t) \cos \theta(t), \quad v_{y\text{Ref}}(t) = v(t) \sin \theta(t) \quad (18)$$

$$x_{\text{Ref}} = \int v_{x\text{Ref}} \cdot dt, \quad y_{\text{Ref}} = \int v_{y\text{Ref}} \cdot dt$$

### 4.5 Simulation Results

To illustrate the ability of the above model in generating practicable paths we generate the path in figure 3a. The limitations of class 2 type paths are demonstrated in the simulation of the forces generated by a WMR tracking the path using [9].

### 5. Continuous Curvature Paths

A clothoid curve has curvature that is proportional to the length along the curve, and is given by,  $Cv(s) = k \cdot s + Cv_0$ , where  $s$  is the length,  $Cv(s)$  the curvature and  $k$  the coefficient or sharpness.

The direction of the tangent vector is the integration of the curvature, and is expressed as,

$$\theta(s) = \int_0^s (k \cdot s + Cv_0) \cdot ds = \frac{1}{2} k \cdot s^2 + Cv_0 \cdot s + \theta_0 \quad (19)$$

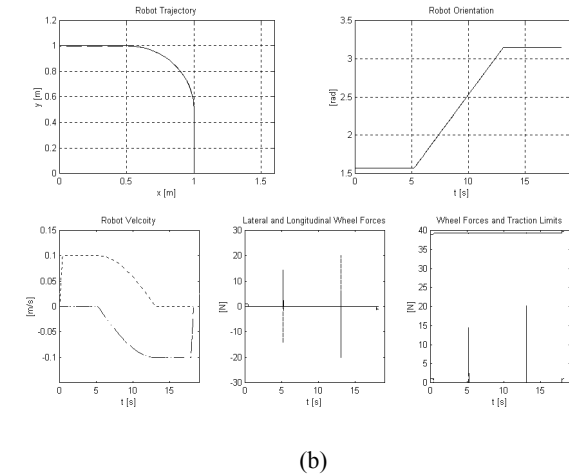
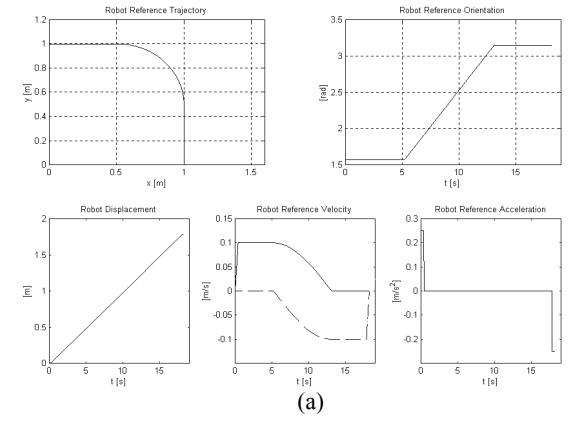


**Figure 3 (a). Type 2 path generation and (b) dynamic simulation of tracking control**

The  $x$  and  $y$  coordinates in terms of the orientation  $\theta$  with initial states  $Cv_0 = \theta_0 = x_0 = y_0 = 0$  are (20),

$$x(\theta) = \frac{1}{\sqrt{2.k}} \int_0^\theta \frac{\cos(\theta)}{\sqrt{\theta}} .d\theta, \quad y(\theta) = \frac{1}{\sqrt{2.k}} \int_0^\theta \frac{\sin(\theta)}{\sqrt{\theta}} .d\theta \quad (20)$$

The right hand side of these equations is called the Fresnel Integration. No analytic solutions exist for either the sine or cosine Fresnel Integrals, hence to calculate their value a numerical integration must be performed which can often be computationally inefficient for real time path generation. To overcome this power series expansions are a feasible alternative for approximating the sine and cosine integrals. The x and y coordinates at each point on the curve can be approximated by the following expressions (21)

$$\begin{aligned} x(\theta) &\approx \sqrt{\frac{2\theta}{k}} \cdot \exp\left(\frac{-\theta^2}{10}\right), \\ y(\theta) &\approx \sqrt{\frac{2}{k}} \cdot \frac{\theta^{3/2}}{3} \exp\left(\frac{-\theta^2}{14}\right) \end{aligned} \quad (21)$$

### 5.1 Continuous Curvature Path Planning

For planning smooth continuous curvature paths a double clothoid (or clothoid pair) can be utilised. The clothoid pair consists of two clothoid curves that are connected at each curve's point of maximum curvature with a different sign of sharpness (k) for each curve. With zero curvature at each end of the clothoid pair means that straight lines can be connected with a smooth transition to each path segment.

In defining a clothoid pair segment, in which  $|\Delta\theta|$  is restricted to  $\leq 180$ , it is necessary to specify the radius of curvature  $\rho$  of a circular arc with the same initial posture  $(x_{i,p}, y_{i,p}, \theta_i)$  and final orientation  $\theta_f$  and direction of rotation  $\delta$  as the planned clothoid pair. Additionally, as per circular arcs, equations (1), (4), (6) and (7) are valid for defining the inputs for the clothoid pair.

Consider two lines passing through the final and initial posture coordinates. The coordinates of the point of intersection of the two lines is calculate as,

$$x_c = \frac{x_i \tan \theta_{i,p} - y_i + y_f - x_f \tan \theta_{f,p}}{\tan \theta_{i,p} - \tan \theta_{f,p}} \quad (22)$$

$$k = \left[ \frac{C_1(\theta_c) (\sin \theta_{i,p} - \cos \theta_{i,p} \tan \psi) + \text{sign}(\Delta\theta_p) S_1(\theta_c) (\cos \theta_{i,p} + \sin \theta_{i,p} \tan \psi)}{x_i (\tan \psi - \tan \theta_{i,p}) - y_i + x_i \tan \theta_{i,p} + y_c - x_c \cdot \tan \psi} \right]^2 \quad (25)$$

$$k = \Phi^2 \left[ \begin{aligned} &C_1(\theta_c) \left( \frac{\sin(\theta_{f,p} + 180) - \cos(\theta_{f,p} + 180) \cdot \tan \psi}{\tan \psi - \tan \theta_{f,p}} \cdot \tan \theta_{f,p} + \sin(\theta_{f,p} + 180) - \sin \theta_{i,p} \right) \\ &- \text{sign}(\Delta\theta_p) S_1(\theta_c) \left( \frac{\cos(\theta_{f,p} + 180) + \sin(\theta_{f,p} + 180) \cdot \tan \psi}{\tan \psi - \tan \theta_{f,p}} \cdot \tan \theta_{f,p} + \cos(\theta_{f,p} + 180) + \cos(\theta_{i,p}) \right) \end{aligned} \right]^2 \quad (26)$$

$$\begin{aligned} y_c &= x_c \tan \theta_{f,p} + y_f - x_f \tan \theta_{f,p} \quad \text{for } |\theta_{i,p}| = 90 \\ y_c &= x_c \tan \theta_{i,p} + y_i - x_i \tan \theta_{i,p} \quad \text{for } |\theta_{i,p}| \neq 90 \end{aligned}$$

In the case where  $|\Delta\theta_p| = 180$  and an actual intersection point does not exist,  $x_c$  and  $y_c$  are calculated as the midpoint along a circular arc joining the final and initial postures such that,

$$\begin{aligned} x_c &= x_i + \rho [\cos \theta_{i,p} + \cos(\theta_{i,p} + 90.\delta)] \\ y_c &= y_i + \rho [\sin \theta_{i,p} + \sin(\theta_{i,p} + 90.\delta)] \end{aligned} \quad (23)$$

The orientation angle of a bisecting line stemming from the point of intersection is defined as,

$$\psi = \theta_{i,p} + \text{sign}(\Delta\theta_p) \cdot (90 + |\Delta\theta_p / 2|) \quad (24)$$

The sharpness (k) influences the shape of the path and hence the start and end coordinates of the clothoid pair which may not necessarily coincide with the end point of the existing segment. By using a circular arc to plan the clothoid path the required sharpness coefficient can be automatically generated to satisfy the path requirements. Using equations (22) – (24) the sharpness becomes equation (25) where  $C_1(\theta_c)$  and  $S_1(\theta_c)$  are  $x(\theta)\sqrt{k}$  and  $y(\theta)\sqrt{k}$  evaluated at  $\theta_c = |\Delta\theta_p / 2|$ , the angle at the point where the two clothoid segments meet. Furthermore when  $|\theta_{p,i}| = 90$ , using equations (22) – (24) the sharpness (k) becomes equation (26) where  $\Phi$  is,

$$\Phi = - \frac{\tan \theta_{f,p} \cdot (y_f - x_f \tan \theta_{f,p} - y_c + x_c \tan \psi)}{\tan \psi - \tan \theta_{f,p} + y_i - y_f + x_f \tan \theta_{f,p}}$$

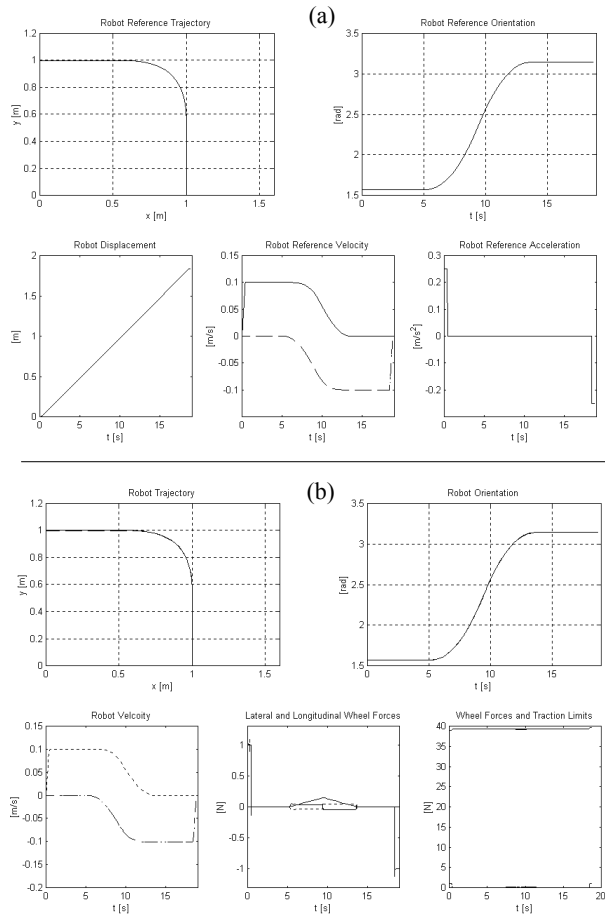


**Figure 4. (a) Type 3 path generation and (b) dynamic simulation of tracking control**

From equations (41) and (42) the total distance  $s$  is simply calculated by  $s = 2 \cdot \sqrt{|\Delta\theta_p|/k}$ .

## 5.2 Continuous Curvature Trajectory Planning

Using the distance function the path planning data is generated based on  $\theta(t)$ . For  $s(t) \leq \sqrt{|\Delta\theta_p|/k}$ ,

$$\theta(t) = \frac{\text{sign}(\Delta\theta) \cdot a \cdot s^2(t)}{2} + \theta_{i,p} \quad (27)$$

where  $s(t) = 2 \cdot \sqrt{|\Delta\theta_p|/k} - s(t)$  for  $s(t) > \sqrt{|\Delta\theta_p|/k}$ .

For  $|\Delta\theta_p| = 180^\circ$ ,  $\delta$  is used in the place of  $\text{sign}(\Delta\theta)$  in (27). The path data is calculated from (18).

## 5.3 Simulation Results

From the model developed in section 5, the class 3 path in figure 4 is generated and the forces of a WMR tracking the path are simulated. Eliminating the discontinuities occurring at the transitions in the class 2 path, significantly reduces the wheel forces.

## 6. Conclusions

In this work techniques have been developed and path generation software implemented for the specification of type 2 and type 3 paths. Moreover, simulation results were presented for the dynamic forces of a WMR demonstrating that the discontinuities occurring at the transitions between straight-line and arc segments of class 2 paths invoke the dynamics of the robot increasing the potential for wheel slip and tracking errors. Class 3 paths are the smoothest and most suitable for WMR path planning having tangent direction and curvature continuity, reducing wheel forces and improving tracking control and performance.

## 7. References

- [1] A. Segovia, M. Rombaut, A. Preciado, and D. Meizel, "Comparative Study of the Different Methods of Path Generation for a Mobile Robot in a Free Environment," *IEEE Int. Conf. on Advanced Robotics*, vol. 2, 1991, pp. 1667–1670.
- [2] T. J. Graettinger and B. H. Krogh, "Evaluation and Time-Scaling of Trajectories for Wheeled Mobile Robots," *Trans. of ASME Journal of Dynamic Sys., Measurement and Control*, vol. 111, June 1989, pp. 222–231.
- [3] Y. Kanayama, A. Nilipour and C. A. Lelm, "A Locomotion Control Method for Autonomous Vehicles," pp. 1315–1317.
- [4] L. E. Dubins, "On Curves of Minimal Length with a Constraint on Average Curvature, and with Prescribed Initial and Terminal Positions and Tangents," *American Journal of Mathematics*, vol. 79, 1957, pp. 497-516.
- [5] W. L. Nelson, "Continuous Steering-Function Control of Robot Carts," *IEEE Transactions on Industrial Electronics*, vol. 36, no. 3, August 1989, pp. 330-337.
- [6] Y. Kanayama and B. I. Hartman, "Smooth Local Path Planning for Autonomous Vehicles," *Proc. IEEE Int. Conf. on Robotics and Automation*, vol. 3, 1989, pp. 1265-1270.
- [7] Y. Konishi and H. Takahashi, "Autonomous Loading of Rocks by use of Intelligent Loaders with a Vision System".
- [8] Y. Kanayama and N. Miyake, "Trajectory Generation for Mobile Robots," *3<sup>rd</sup> International Symposium on Robotics Research*, pp. 333-340.
- [9] J Garbutt, T Vinay, S John (2003), "Establishing Limits Kinematic Based Control for Wheeled Mobile Robots", Proceedings of the Int. Conference on Machine learning: Models, Technologies & Applications. Las Vegas, Nevada, USA, CSREA press, pg 197-202, ISBN 1 932415 11 4.